Luminal pulse velocity in a superluminal medium

Heisuke Amano and Makoto Tomita

Department of Physics, Faculty of Science, Shizuoka University, 836, Ohya, Suruga-ku, Shizuoka 422-8529, Japan

To investigate the physical meaning of pulse peak in fast and slow light media, we investigated propagation of differently shaped pulses experimentally, controlling the sharpness of the pulse peak. Symmetric behavior with respect to fast and slow light was observed in traditional Gaussian pulses; that is, propagated pulses were advanced or delayed, respectively, whereas the pulse shape remained unchanged. This symmetry broke down when the pulse peak was sharpened; in the fast light medium, the sharp pulse peak propagated with luminal velocity, and the transmitted pulse deformed into a characteristic asymmetric profile. In contrast, in the slow light medium, a time-delayed smooth peak appeared with a bending point at $t = 0$. This symmetry breaking with respect to fast and slow light is a universal characteristic of pulse propagation in causal dispersive systems. The sharp pulse peak can be recognized as a bending nonanalytical point and may be capable of transferring information.

I. INTRODUCTION

The problems surrounding the physical meaning of pulse peaks in optical pulses have long been debated, especially for fast light media. In anomalous dispersion regions, a pulse peak can propagate with superluminal or even negative velocities [1–7]. Such velocities seemingly contradict the theory of special relativity, however, it is now understood that the superluminal velocity of a smooth Gaussian-shaped pulse peak does not violate causality; the arrival of the smooth pulse peak can be predicted on the basis of the expansion of the leading part of the pulse, and hence the pulse peak does not contain true information [8–10]. Furthermore, it has been experimentally demonstrated that a Gaussian-shaped peak exits from the far side of a superluminal medium, even though the incident pulse terminates at a time before the Gaussian pulse peak enters the medium [11].

Historically, Sommerfeld and Brillouin showed that the main body of a pulse propagates through the medium with a group velocity, whereas the front edges of the precursors always travel at c, the velocity of light in a vacuum [1]. This idea has been developed to incorporate the fact that true information is encoded on nonanalytical points or singularities along the wave packets [12–15]. As expansion of the leading part of the pulse cannot be applied beyond nonanalytical points, the arrival of pulse points after the nonanalytical point is considered a new signal. Practically, the definition of the information velocity incorporates many factors [16–19]. In the presence of quantum noise associated with the amplifying medium, a larger signal is required to achieve a given signal-to-noise ratio at the output, hence the arrival of the signal is significantly retarded [13,16,19]. This retardation has been found in numerical simulations to be larger than the reduction in propagation time due to anomalous dispersion.

Nonanalytical points, as information carriers, are not restricted to the front of the pulse or discontinuous points in the pulse envelope. A sharp bending point, at which the envelope function is continuous but the derivatives are discontinuous, could also act as a nonanalytical point [20]. Propagation of bending nonanalytical points encoded on temporally Gaussian-shaped optical pulses was recently investigated in

fast and slow light systems. It was shown that the propagation of the bending nonanalytical point was in accordance with the causal principle [21].

Our motivation here is to clarify the physical meaning of the pulse peak in fast and slow light media. If the pulse has a sufficiently sharp peak, such a peak could be recognized as a bending nonanalytical point. The pulse peak could then transfer information. The influence of pulse shape on pulse propagation in a superluminal medium is systematically investigated, particularly the sharpness of the pulse peak. Although pulse propagation through resonant media has been widely studied, there is no systematic data on the effect of input pulse shape.

For traditional Gaussian pulses, transmitted pulses were formed such that the delay times were symmetrically negative and positive in fast and slow light media, respectively, whereas the pulse shape was unchanged. When the pulse peak was sharpened, this symmetry broke down. In the fast light medium, the sharply peaked input pulses propagated with luminal velocity rather than group velocity, and the transmitted pulse deformed into a characteristic asymmetric profile. In contrast, in the slow light medium, the sharply peaked input pulse produced a relatively smooth output pulse peak with a positive time delay. A bending point also appeared at $t = 0$. The experimental results were analyzed considering the pulse peak as a nonanalytical point. Universal characteristics of pulse propagation in causal dispersive systems are discussed.

II. PULSE SHAPES

A number of experimental and theoretical investigations have been reported on pulse propagation in resonant media. The temporal functional forms of the input pulses were, however, very limited; in most cases, Gaussian pulses were considered. From an experimental point of view, pulses naturally obtainable from instruments can frequently be approximated as Gaussian pulses. For Gaussian pulses, the effect of group velocity dispersion broadens the pulse duration while maintaining the pulse shape. Gaussian pulses may thus be suitable for experiments on pulse peak propagation. Another functional form sometimes used is square-modulated

pulses. Summerfield and Brillouin examined the propagation of square-modulated pulses on the basis of the saddle-point method and investigated the effect of optical precursors [1]. This type of square-modulated pulse was also employed in recent experiments on precursors in electromagnetically induced transparency [22–24] as well as coupled resonator-induced transparency [25]. Single-side exponential pulses have also been used successfully to examine both the precursors and the propagation of the main body of pulses simultaneously [26].

In our experiments, we used the following functional form for the slowly varying envelope of the input pulses:

$$f(t) = A \, \exp\left[-\left| \frac{t}{t_p} \right|^\alpha \right], \tag{1}$$

where A and t_p represent the pulse amplitude and temporal duration, respectively. The parameter α indicates the sharpness of the peak. For $\alpha = 1$, the pulse is exponential on both sides, and, in this case, the pulse peak is mathematically a nonanalytical point $\lim_{x \to -0}(df/dx) \neq \lim_{x \to +0}(df/dx)$ in Eq. (1). As α increases the pulse peak becomes smoother; pulses of this functional form are an extension of traditional Gaussian-shaped pulses, which arise for the specific case where $\alpha = 2$. In this case, both the function and the derivatives are continuous at the peak. When α exceeds $2 (\alpha > 2)$, the pulse peak becomes flattened, compared with the Gaussian pulse.

III. EXPERIMENT

The inset in Fig. 1 shows the experimental setup. Fiber ring resonators were used for the fast and slow light media, which offer highly controllable dispersion through cavity loss x and the coupling strength between the fiber and the ring resonator y. Note that our interest here lies in the influence of pulse shape on pulse propagation and not in the dispersion characteristics of the ring resonators, which have been studied extensively. The stationary input-output characteristics of the resonator can
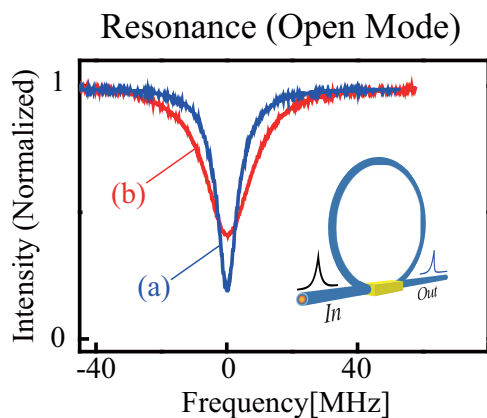

FIG. 1. (Color online) Schematic of the experimental setup (inset). In and out correspond to the input and output (transmitted) pulses, respectively. The blue (a) and red (b) solid curves are experimental observations of the resonance spectra for undercoupling and overcoupling conditions, i.e., fast and slow light media, respectively. The resonance widths were 7.6 and 11.4 MHz, respectively.

be analyzed based on directional coupling theory [27,28]. The transmitted light intensity $T(\omega)$, as a function of frequency ω, shows a periodic dip due to the resonances. The dispersion relationship depends on the loss x and coupling strength y. For undercoupling conditions $(x < y)$, the transmission phase as a function of frequency $\theta(\omega)$ shows an anomalous dispersion at the center of the resonance. The group delay is expected to be negative $\tau_g = \partial\theta/\partial\omega < 0$, corresponding to superluminal pulse propagation, i.e., fast light. In contrast, for overcoupling conditions $(x > y)$, the transmission phase shows normal dispersion $\partial\theta/\partial\omega > 0$, and one would expect slow light [28]. In the current study, 90:10 $(y^2 = 0.90)$ and 80:20 $(y^2 = 0.80)$ couplers were used to achieve undercoupling and overcoupling conditions, respectively. We inserted an additional loss element within the ring resonator to control the loss parameter $(x^2 = 0.89)$. The physical length of the ring was $L_R = 200$ cm. An Er-fiber laser was used as the incident light source. The spectral width was 1 kHz, and the laser frequency was tuned by piezoelectric control of the cavity length. A series of pulses of the temporal functional form of Eq. (1) were prepared by a computer program. The optical pulses were then generated using a 240-MHz function generator and a 10-GHz LiNbO$_3$ (LN) modulator. The repetition rate was 100 kHz, and the incident power was 0.1 mW. Transmission intensity through the system was observed using an InGaAs photodetector and recorded using a 600-MHz digital oscilloscope.

The blue and red curves in Fig. 1 are the observed resonance spectra as a function of the detuning frequency for undercoupling and overcoupling conditions, respectively. These spectra were observed in the continuous-wave mode in which the LN modulator was operated in the open mode. The transmitted light intensity $T(\omega)$ showed a dip due to the resonance. The resonance widths were $\delta\nu_R = 7.6$ and 11.4 MHz, respectively. We systematically examined the propagation of pulses of different values of α in Eq. (1) under resonant conditions.

Figure 2 shows the experimentally observed transmitted temporal pulse profiles through the ring resonators. The left column shows the input pulses with the pulse shape controlled through the parameter α. The middle column is the transmitted temporal pulse profiles through the undercoupling ring resonator, i.e., the fast light medium. For the pulse with $\alpha = 1$ (exponential on both sides), the pulse peak showed almost no delay and appeared at the same time as under off-resonance conditions [Fig. 2(a2)]. This indicates that the pulse peak propagated with luminal velocity as opposed to group-velocity propagation. The transmitted pulse profile reshaped and deformed into a characteristic asymmetric profile with respect to the peak position. The section after the peak showed a greater reduction compared with the first part of the pulse. With increasing α, $1 < \alpha < 2$, the peak in the input pulses became smooth. The peak in the output pulses advanced gradually, and the pulse shape recovered symmetry with respect to the pulse peak [Figs. 2(b2)–2(d2)]. In the present experiments, the peak was still sharp, hence the ring resonator could not respond to the peak. For traditional Gaussian-shaped pulses, i.e., $\alpha = 2$, the transmitted pulse was nearly symmetric with respect to the peak, and the peak advanced by $\tau = -63$ ns, which is in good agreement with the theoretically expected
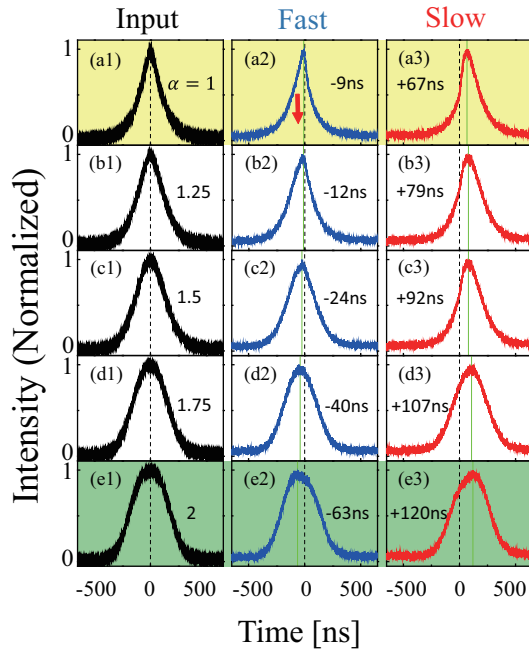
FIG. 2. (Color online) Experimental observations of the transmitted temporal pulse profiles. The left column shows the input pulses. The middle and right columns are transmitted pulse profiles through undercoupled and overcoupled resonators, i.e., fast and slow light media, respectively. The parameter α was (a) 1.0, (b) 1.25, (c) 1.5, (d) 1.75, and (e) 2.0. The condition $\alpha = 1.0$ corresponds to a pulse that is exponential on both sides (light yellow hatching), and $\alpha = 2.0$ corresponds to a traditional Gaussian pulse (light green hatching). The pulse peaks of Gaussian pulses showed negative delays of (e2) -63 ns and positive delays of (e3) 120 ns with undercoupling and overcoupling conditions, respectively. The vertical green lines indicate the peak position. The downward arrow in (a2) shows the centroid of mass of the transmitted pulse profile. To see the pulse shape clearly, all intensities were normalized with respect to the maximum of the pulses.

value of the group delay for the undercoupled ring resonator $\tau_g = -64$ ns [Fig. 2(e2)].

The right column in Fig. 2 shows the transmitted temporal pulse profiles in the overcoupled ring resonator, i.e., the slow light medium. In this case, in contrast to the results from the undercoupled ring resonator [Fig. 2(a2)], the transmitted pulse from the overcoupled ring resonator was accompanied by a relatively smooth pulse peak with a large delay time of $\tau = 67$ ns, even with the sharp input pulse defined by $\alpha = 1$ [Fig. 2(a3)]. It is also notable that a bending point appeared at $t = 0$. This bending point is related to the sharp peak in the input pulse. As α increased over the range of $1 < \alpha < 2$, the delay time increased, and the bending point at $t = 0$ weakened. For the traditional Gaussian-shaped pulse, i.e., $\alpha = 2$, the pulse was nearly symmetric, and the pulse peak showed a delay of $\tau_g = 120$ ns [Fig. 2(e3)]. Comparing Figs. 2(e2) and 2(e3), we see that the behaviors of the transmitted pulses were symmetric with respect to the fast and slow light media; the delay times were negative [Fig. 2(e2)] and positive [Fig. 2(e3)], respectively, and the pulse shape was unchanged. The observed delay times of the pulse peak as a function of the parameter α are summarized in Fig. 3. The blue closed and red open
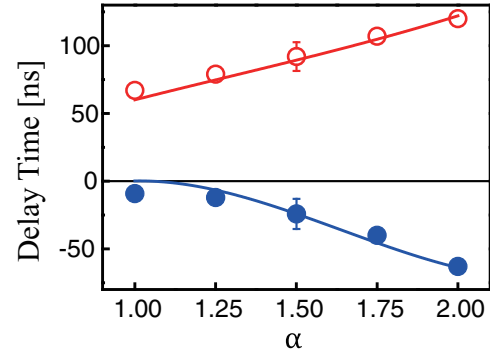

FIG. 3. (Color online) Delay time of the pulse peak as a function of the parameter α. The blue solid and red open circles are experimentally observed delay times. The red and blue curves are the calculated delay times given undercoupling and overcoupling conditions, respectively.

circles represent the delay times for the undercoupled and overcoupled ring resonators, respectively.

IV. SIMULATION

To analyze the results of the experiments, we simulated the propagation of pulses of different shapes. Figure 4 shows the calculated curves of transmitted pulse profiles with different values of α. In addition to the experimental values of α, regions where $\alpha < 1$ and $\alpha > 2$ were also investigated. The middle and right columns in Fig. 4 show calculated curves for the transmitted pulses for undercoupling and overcoupling conditions, i.e., fast and slow light media, respectively. Simulation results correlated well with experimental observations. In the fast light system, for $\alpha = 1$, the pulse peak appeared immediately as the pulse entered the system [Fig. 4(b2)]. The transmitted pulse profile reshaped and deformed into the characteristic asymmetric shape. For $\alpha = 1$, the pulse peak is mathematically a nonanalytical point. The peak could carry information [12,20,21] and, hence, should propagate with a velocity slower than c, in accordance with the requirement of relativistic causality. With increasing α from 1 to 2, the peak gradually advanced, and the transmitted pulse profile recovered symmetry. For a traditional Gaussian pulse, i.e., $\alpha = 2$, the transmitted pulse profile was perfectly symmetric, and the pulse peak showed a negative delay of $\tau_g = -64$ ns [Fig. 4(f2)]. For the slow light system, the simulation results also correlated with the main features of the experimental results. Even with a sharp pulse of $\alpha = 1$, a smooth pulse peak appeared with a positive delay. The input pulse peak acted as a nonanalytical point, generating a bending point and a steep rise at $t = 0$ in the transmitted pulse [Fig. 4(b3)].

The features observed in the simulations were confirmed in the Fourier spectra of the input pulses used in the simulation (Fig. 5). The spectra consisted of a main part associated with the main body of the pulse and broadband wings related to the sharp peak. We denote the width of these components as $\delta\nu_{main}$ and $\delta\nu_p$, respectively. For $\alpha = 1$, the broadband wing frequency components lay outside the resonance $\delta\nu_p \gg \delta\nu_R$ [Fig. 5(b)]; the resonator could not respond to these broadband frequencies. As a result, the pulse propagated through the
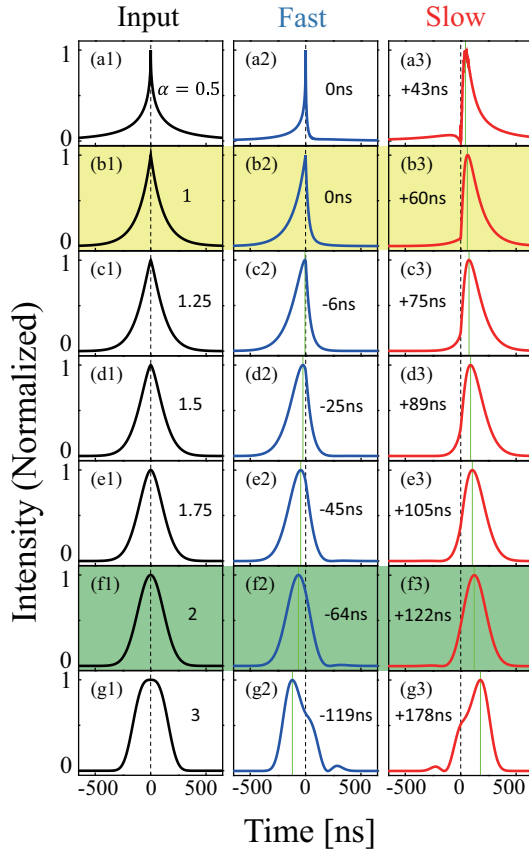
FIG. 4. (Color online) Calculated curves for the transmitted pulse profiles. The left column shows the input pulses. The middle and right columns show the transmitted pulse profiles for undercoupling and overcoupling conditions, i.e., fast and slow light media, respectively. The parameters α were (a) 0.50, (b) 1.0, (c) 1.25, (d) 1.5, (e) 1.75, (f) 2.0, and (g) 3.0.

system as if the medium was empty. In the fast light medium, the peak propagated with luminal velocity. In the slow light medium, the broadband components produced a bending point at $t = 0$. As α increased and the pulse peak gradually became smooth, the frequency wings of the spectrum shrank [Fig. 5(c)]. In the region $1 < \alpha < 2$. The spectral tail related to the peak was still broad as $\delta\nu_p \geqslant \delta\nu_R$, and the delay time was smaller than τ_g. When $\alpha = 2$, the spectrum resided in the anomalous region of the undercoupled ring resonator. The smooth Gaussian pulse peak propagated with superluminal group velocity without significant deformation. As α increased further beyond $\alpha > 2$, the transmitted pulse profile suffered serious deformation [Figs. 4(g2)] and 4(g3)]. In this region, the pulse peak became flattened [Fig. 4(g1)]. Figure 5(d) shows the Fourier spectrum of the pulse formed at $\alpha = 3$; the main body of this pulse had a broader spectral width $\delta\nu_{\mathrm{main}} \geqslant \delta\nu_R$, and the pulse shape showed significant deformation.

Our simulation results correlated well with experimental observations; however, several differences were evident. In the experimental results shown in Fig. 2(a2), the pulse peak showed a slight negative delay (-2 ns), even with the pulse formed at $\alpha = 1$. In contrast, the simulation showed a zero delay time $\tau = 0$ in accordance with the fact that the pulse

peak was a nonanalytical point. The slight negative delay observed in our experiments could be attributed to the finite time resolution of the experimental system. A mathematical or ideal nonanalytical point localizes at an infinitesimal time point, hence, requires an infinite bandwidth. In this case, the point acts nonanalytically for any dispersive system. However, physical systems have finite bandwidths; therefore, the experimental nonanalytical point has a finite time duration. The experimental time resolution of our pulse generation system, including the function generator and LN modulator, was $\delta\nu_{\mathrm{gen}} \sim 240$ MHz. The time resolution of the observation system, including the detector and digital oscilloscope, was up to $\delta\nu_{\mathrm{obs}} \sim 600$ MHz. The resonance width of the resonator was $\delta\nu_R \sim 6$ MHz. Therefore, the present input pulse peak emulated a nonanalytical point fairly well for the resonator; however, the pulse sharpness was insufficient to be recognized as a perfect nonanalytical point $\delta\nu_{\mathrm{obs}} \geqslant \delta\nu_{\mathrm{gen}} \gg \delta\nu_R$.

V. DISCUSSION

A. Causal symmetry breaking

For the traditional Gaussian pulses ($\alpha = 2$), the transmitted pulses were symmetrically formed with respect to fast and slow light; i.e., the delay times were negative [Figs. 2(e2) and 4(f2)] and positive [Figs. 2(e3) and 4(f3)], respectively, and the pulse shapes were symmetric with respect to the peak. This symmetry broke down in the sharp pulses formed when $\alpha = 1$. For fast light, the pulse peak showed no delay, and the transmitted pulse profile deformed into an asymmetric shape [Figs. 2(a2) and 4(b2)]. In contrast, for slow light, a relatively smooth pulse peak appeared with a large positive delay with a bending point at $t = 0$ [Figs. 2(a3) and 4(b3)]. The behaviors of the fast and slow light could be a universal characteristic of real causal dispersive systems. To confirm this universality, we also calculated propagation of pulses in which both sides were exponential, i.e., $\alpha = 1$, through a Lorentz medium. The spectral form was assumed to be $g(\omega) = \beta/[(\omega - \omega_0) - i\gamma]$, where ω_0 is the resonant frequency, β is a constant that reflects the light-matter interaction. $\beta > 0$
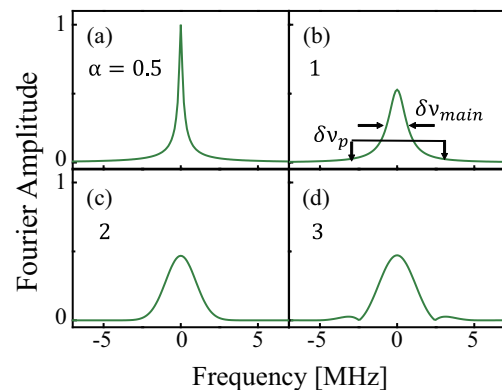

FIG. 5. (Color online) Absolute values of the amplitudes of the Fourier components of the input pulses for different values of α: (a) 0.5, (b) 1.0, (c) 2.0, and (e) 3.0. The spectra consist of a main section associated with the main body of the pulse $\delta\nu_{\mathrm{main}}$, and the broadband wings are related to the sharp pulse peak $\delta\nu_p$. Amplitudes are normalized with respect to the height of the $\alpha = 0.5$ spectrum.
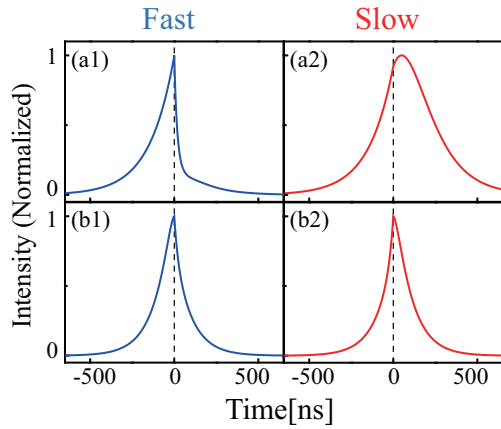
FIG. 6. (Color online) Calculated curves for the transmitted pulse profiles. The input pulse is the same as that shown in Fig. 4(b1), i.e., exponential on both sides. The left and right columns correspond to fast and slow light media. (a1) and (a2) are the transmitted pulse profiles through Lorentz-shaped absorbing and amplifying media under resonant conditions, respectively, where $\omega_0 = 2.0 \times 10^{14}, \beta = 5.0 \times 10^3$, and $\gamma = 3.0 \times 10^7$ Hz and the propagation distance $z = 0.03$ m. (b1) and (b2) are the transmitted pulse profiles through the virtual dispersive system. The transmitted pulse profiles are symmetric with respect to the fast and slow light systems.

and $\beta < 0$ correspond to absorbing and amplifying media [29], which show anomalous and normal dispersions at the resonance frequency $\omega = \omega_0$, respectively. Figures 6(a1) and (a2) show the transmitted pulse profile for the absorbing and amplifying Lorentz media, respectively. Given that the incident pulse was exponential on both sides through the absorbing and amplifying media, the transmitted pulse exhibited similar behaviors as observed via the undercoupled and overcoupled ring resonators, respectively. This supports the hypothesis that the symmetry breaking observed when $\alpha = 1$ in the fast [Figs. 4(b2) and 4(b3)] and slow [Figs. 4(f2) and 4(f3)] light media is an intrinsic feature of causal dispersive systems. In the amplifying Lorentz line, the normal dispersion delays the pulse. Simultaneously, from the Kramers-Kronig relation, this normal dispersion should be accompanied by amplification; hence, the delayed part of the pulse would be strongly enhanced. In this case, a delayed isolated smooth pulse peak appeared in the transmitted pulse profile [Fig. 4(f3)].

We also used a virtual dispersive system in which the imaginary part of the response function was set to 1, whereas for the real part of the response function that of the undercoupled and overcoupled ring resonators were used. Although such a system does not satisfy the Kramers-Kronig relation and hence cannot be realized in a real system, it is instructive to examine pulse propagation through this noncausal system. Figures 6(b1) and 6(b2) show the transmitted pulse profiles for the virtual fast and slow light media, respectively. In this case, the transmitted pulse shapes were symmetric with respect to the fast and slow light, both having pulse peaks at $t = 0$. Causal symmetry breaking does not take place. These results are in good agreement with the idea that the symmetry breaking observed for $\alpha = 1$ with respect to fast and slow light is a consequence of the causal nature of real systems.

B. Superluminal centroid velocity

The sharp pulse peak with $\alpha = 1$ propagates with luminal velocity even in the fast medium. There is another definition of propagation velocity, which describes the motion of the pulse based on the centroid of mass [30,31]. The centroid of mass is defined as the time expectation integral over the Poynting vector. It has been suggested that the interval of the time expectations integral calculated at the starting and
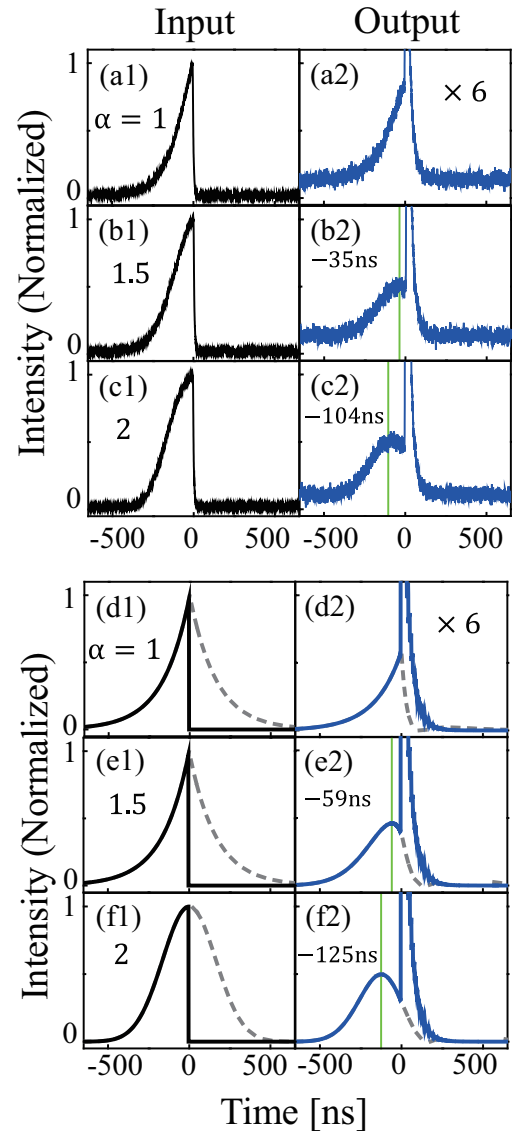

FIG. 7. (Color online) Transmitted pulse profile through the undercoupled ring resonator (fast light) obtained using the peak-truncated input pulses. The input pulses were truncated at $t_R = -6$ ns before the peak of the original pulses. (a)–(c) Experimental observations. (d)–(f) Calculated curves corresponding to the graphs in (a)–(c), respectively. The solid black curves in the left columns are peak-truncated input pulses. The solid blue curves in the right columns are the output pulses through the ring resonator that correspond to the truncated input in the left column. The parameter α is (a) 1.0, (b) 1.5, and (c) 2.0. For comparison, the dashed-black curves in (d)–(f) represent the original input and output pulses without pulse peak truncation.

arrival points can be separated into the sum of the net group delay and the reshaping delay. Net group delay is given by the spectral superposition of the group delay. The reshaping delay is the difference in arrival time at the initial point without and with the spectral amplitude that is attenuated or amplified during propagation. The propagation velocity, in terms of the net group and reshaping delays, is always significant, even in cases of strong distortion [31]. In our experiments, we prepared input pulses by slicing out the pulse envelope from a coherent continuous wave; hence, the pulses had no initial phase modulation. In this case, the reshaping delay was negligible, and only the net group delay was relevant for describing the propagation velocity. The arrow in Fig. 2(a2) shows the centroid of mass of the transmitted pulse, which shows a negative delay of $\tau_c = -18$ ns. Although the Fourier spectrum of the sharp pulse with $\alpha = 1$ had broadly spread tails $\delta \nu_p > \delta \nu_R$, the main components of the frequency lay within the anomalous dispersion region $\delta \nu_{main} < \delta \nu_R$; hence, the net delay had a negative value. Although the centroid of mass velocity can be superluminal or negative, it is apparent that the centroid of mass cannot transfer information superluminally because the position of the centroid can be calculated only after the entire pulse has arrived.

C. Peak-truncation experiments

The peak of Gaussian-shaped pulses is an analytic continuation over time of the earlier portion of the input pulse envelope. The superluminal pulse peak in the fast light medium is not information. It was experimentally demonstrated that a Gaussian-shaped peak $\alpha = 2$ exited from the far side of a superluminal group-velocity medium, even though the incident pulse was terminated before its peak [11]. We performed similar experiments using truncated pulses of different values of α. First, we review the results with peak-truncated Gaussian pulses. The solid blue line in Fig. 7(c2) shows the experimental results obtained with traditional Gaussian pulses after being injected with the input pulse truncated at $\tau_R = -6$ ns. A smooth peak emerged at the output. The output peak for the truncated pulse has the same advancement τ_g as the original Gaussian pulse. Figure 7(a2) shows a similar experiment for the case where $\alpha = 1$. In this case, a large kick was observed at

the truncating point, similar to that observed with a Gaussian pulse. The pulse peak, however, did not appear in the output because the arrival of the sharp pulse peak cannot be predicted by the analytic continuation of the leading part of the pulse. It is interesting to examine whether we could observe the peak in the output pulse for the pulses where $\alpha = 1.5$, which showed a rather small advancement compared with Gaussian pulses. The experimental results in Fig. 7(b2) indicate that the pulse peak can be observed, insofar as the truncating point lies in the region of $\tau < t_R \leqslant 0$, even though the pulse shape was not Gaussian. These experimental results are in good agreement with the causal principle of information transfer in fast light systems [8,9,11,12].

VI. SUMMARY

We investigated the propagation of differently shaped pulses, controlling the sharpness of the pulse peak. For traditional Gaussian pulses, the transmitted pulses were symmetrically formed with respect to fast and slow light. When the pulse peak was sharpened, this symmetry broke down. Specifically, in the fast medium, the pulse peak propagated, not with the group velocity, but with luminal velocity, exhibiting an asymmetric shape. In contrast, in the slow light medium, a time-delayed smooth pulse peak appeared. The experimental results indicate that when the pulse has a sufficiently sharp peak, the pulse peak should be recognized as a nonanalytical point. The sharp pulse peak could carry information in the same way as the pulse front. The sharply peaked pulse may also be useful in applications requiring precise optical measurement to avoid higher-order dispersions or complicated spectral structures in the system through which the pulse propagates. It may be interesting to investigate the operational information velocity defined relevant to the sharp pulse peak and the retardation of the signal in the presence of detector noise or quantum fluctuations. Although we utilized the functional form of Eq. (1) for the purpose of extension of the traditional Gaussian-shaped pulses, other shapes may also be of interest.

ACKNOWLEDGMENT

[1] L. Brillouin, *Wave Propagation and Group Velocity* (Academic, New York, 1960).

[2] Focus issue, "Slow light," Nat. Photonics **2**, 447 (2008).

[3] P. W. Milonni, *Fast Light, Slow Light and Left-Handed Light* (Taylor & Francis, New York, 2004).

[4] S. Chu and S. Wong, Linear Pulse Propagation in an Absorbing Medium, Phys. Rev. Lett. **48**, 738 (1982).

[5] L. J. Wang, A. Kuzmich, and A. Dogariu, Gain-assisted super-luminal light propagation, Nature (London) **406**, 277 (2000).

[6] M. A. I. Talukder, Y. Amagishi, and M. Tomita, Superluminal to Subluminal Transition in the Pulse Propagation in a Resonantly Absorbing Medium, Phys. Rev. Lett. **86**, 3546 (2001).

[7] G. M. Gehring, A. Schweinsberg, C. Barsi, N. Kostinski, and R. W. Boyd, Observation of backward pulse propagation through a medium with a negative group velocity, Science **312**, 895 (2006).

[8] G. Diener, Superluminal group velocities and information transfer, Phys. Lett. A **223**, 327 (1996).

[9] K. Wynne, Causality and the nature of information, Opt. Commun. **209**, 85 (2002).

[10] B. Macke and B. Segard, Propagation of light-pulses at a negative group-velocity, Eur. Phys. J. D **23**, 125 (2003).

[11] M. Tomita, H. Amano, S. Masegi, and A. I. Talukder, Direct Observation of a Pulse Peak Using a Peak-Removed Gaussian

Optical Pulse in a Superluminal Medium, Phys. Rev. Lett. **112**, 093903 (2014).

[12] J. C. Garrison, M. W. Mitchell, R. Y. Chiao, and E. L. Bolda, Superluminal signals: causal loop paradoxes revisited, Phys. Lett. A **245**, 19 (1998).

[13] M. D. Stenner, D. J. Gauthier, and M. A. Neifeld, The speed of information in a 'fast-light' optical medium, Nature (London) **425**, 695 (2003).

[14] M. D. Stenner, D. J. Gauthier, and M. A. Neifeld, Fast Causal Information Transmission in a Medium With a Slow Group Velocity, Phys. Rev. Lett. **94**, 053902 (2005).

[15] M. Tomita, H. Uesugi, P. Sultana, and T. Oishi, Causal information velocity in fast and slow pulse propagation in an optical ring resonator, Phys. Rev. A **84**, 043843 (2011).

[16] A. Kuzmich, A. Dogariu, L. J. Wang, P. W. Milonni, and R. Y. Chiao, Signal Velocity, Causality, and Quantum Noise in Superluminal Light Pulse Propagation, Phys. Rev. Lett. **86**, 3925 (2001).

[17] U. Vogl, R. T. Glasser, and P. D. Lett, Advanced detection of information in optical pulses with negative group velocity, Phys. Rev. A **86**, 031806(R) (2012).

[18] A. H. Dorrah and M. Mojahedi, Velocity of detectable information in faster-than-light pulses, Phys. Rev. A **90**, 033822 (2014).

[19] A. H. Dorrah, A. Ramakrishnan, and M. Mojahedi, Time-frequency dynamics of superluminal pulse transition to the subluminal regime, Phys. Rev. E **91**, 033206 (2015).

[20] R. Y. Chiao and A. M. Steinberg, Tunneling Times and Superluminality, Progress in Optics XXXVII, in *Progress in Optics*, edited by E. Wolf (Elsevier, Amsterdam, 1997), Vol. XXXVII, p. 345.

[21] R. Suzuki and M. Tomita, Causal propagation of nonanalytical points in fast- and slow-light media, Phys. Rev. A **88**, 053822 (2013).

[22] B. Macke and B. Ségard, Optical precursors in transparent media, Phys. Rev. A **80**, 011803(R) (2009).

[23] D. Wei, J. F. Chen, M. M. T. Loy, G. K. L. Wong, and S. Du, Optical Precursors with Electromagnetically Induced Transparency in Cold Atoms, Phys. Rev. Lett. **103**, 093602 (2009).

[24] H. Jeong and S. Du, Two-way transparency in the light-matter interaction: Optical precursors with electromagnetically induced transparency, Phys. Rev. A **79**, 011802(R) (2009).

[25] T. Oishi, R. Suzuki, P. Sultana, and M. Tomita, Optical precursors in coupled-resonator-induced transparency, Opt. Lett. **37**, 2964 (2012).

[26] J. Aaviksoo, J. Kuhl, and K. Ploog, Observation of optical precursors at pulse propagation in GaAs, Phys. Rev. A **44**, R5353 (1991).

[27] K. Totsuka, N. Kobayashi, and M. Tomita, Slow Light in Coupled-Resonator-Induced Transparency, Phys. Rev. Lett. **98**, 213904 (2007).

[28] K. Totsuka and M. Tomita, Slow and fast light in a microsphere-optical fiber system, J. Opt. Soc. Am. B **23**, 2194 (2006).

[29] R. Y. Chiao, Superluminal (but causal) propagation of wave packets in transparent media with inverted atomic populations, Phys. Rev. A **48**, R34(R) (1993).

[30] J. Peatross, S. A. Glasgow, and M. Ware, Average Energy Flow of Optical Pulses in Dispersive Media, Phys. Rev. Lett. **84**, 2370 (2000).

[31] A. I. Talukder, T. Haruta, and M. Tomita, Measurement of Net Group and Reshaping Delays for Optical Pulses in Dispersive Media, Phys. Rev. Lett. **94**, 223901 (2005).